Russian Physics Journal, Vol. 46, No. 6, 2003

PHYSICS AND TECHNOLOGY OF III–V HETEROSTRUCTURES: CURRENT STATUS AND TRENDS IN THE DEVELOPMENT

A. L. Aseev, O. P. Pchelyakov, and A. I. Toropov UDC 621.315.592

Rapid progress in semiconductor electronics and transition from micro- to nanoelectronics result from progressively smaller dimensions of complementary metal-oxide-semiconductor (CMOS) transistors, development of new single-electron devices, and optical and quantum logical elements. The development of nanotechnologies is an integral part of this process. The present paper reviews the current status of research in molecular-beam epitaxy performed at the Institute of Semiconductor Physics of the Siberian Branch of the Russian Academy of Sciences (Novosibirsk).

INTRODUCTION

After pioneer works of J. R. Arthur *et al*. [1], the synthesis of thin films in ultrahigh vacuum (UHV) has occupied a prominent place in semiconductor materials science [2]. The molecular-beam epitaxy (MBE) technique stimulated the emergence and development of a new type of micro-, nano-, and optoelectronic devices based on multilayer epitaxial heterostructures containing superlattices and quantum wires and dots. The quantum properties of the material are used to develop a new generation of microelectronic devices. The advent of semiconductor injection lasers based on quantum wells and dots, transistors with high mobility in the channel, resonance tunnel diodes, and many other devices based on achievements in the band-semiconductor engineering would be simply impossible without the MBE technology. A further development of the MBE technique is stimulated by a common interest in the creation of a quantum computer. Naturally, a means for this development can be provided only through a further improvement in ultrahigh vacuum technique and modernization of analytic equipment. Thirty years of the MBE use for the sophisticated study of the elementary processes proceeding on the growth surface have resulted in the creation of the fundamental database and considerable progress in the development of solid-state physics. Advances in MBE have stimulated a rapid progress in nanotechnologies as well as the mere fact of their emergence.

MBE has allowed unexcelled results to be obtained in large-scale production of multilayer epitaxial structures with smooth atomic heterointerfaces and precision control over the thickness, composition, and doping profile of individual layers to be exercised. However, it should be noted that the cost of heterostructures produced by the MBE technique is higher than the cost of the corresponding structures produced by the widespread technique of film synthesis from the vapor phase. Therefore, a further progress in the industrial MBE technique is associated with an increase of its efficiency.

DEVELOPMENT OF THE MBE TECHNIQUE AT THE ISP SB RAS

The development of MBE at the Institute of Semiconductor Physics of the Siberian Branch of the Russian Academy of Sciences (ISP SB RAS) (Novosibirsk) was initiated by Academician A. V. Rzhanov (1920-2000), the first Director of the ISP SB RAS, and Professor S. I. Stepin (1940-1990), the founder of the Russian School of MBE Physics and Technology. Their roles cannot be overestimated. The first self-made MBE systems were developed at the ISP SB RAS in 1979. Despite being ten years behind the leading industrial countries, the concentration of intellectual, financial, and industrial resources allowed the Institute to develop a multichamber MBE system with comparable parameters in 1992. This system embodied the main design principles of technological MBE machines and the optimal analytic techniques of control

Institute of Semiconductor Physics of the Siberian Branch of the Russian Academy of Sciences. Translated from Izvestiya Vysshikh Uchebnykh Zavedenii, Fizika, No. 6, pp. 21–26, June, 2003.

 1064-8887/03/4606-0537$25.00

over the growth process. The system comprised a module for preparation and quality control of the substrate, a module for synthesis of semiconducting heterostructures, and a module for UHV deposition of metal and dielectric films. Automated systems of control over the production processes were used in all modules.

From the most important analytic equipment, designed and manufactured at the ISP SB RAS, the following should be mentioned:

1. A reflection high-energy electron diffraction (RHEED) system permitting to control the structure and perfection of growing crystal layers and to evaluate their growth rates and composition.

2. A built-in ellipsometer for measuring the thickness and optical characteristics of epitaxial structures, whose original design and software allowed the composition and roughness of films to be controlled together with the temperature of the growing substrate. Ellipsometry essentially expands the capabilities of nondestructive control and is irreplaceable when the RHEED method becomes inapplicable (at high pressures in the growth chamber and high sensitivity of growing layers to irradiation).

3. A polarization pyrometer of original design for contactless control over the temperature of the growth process.

In 1987–1992, 36 MBE systems of various configurations, more than 100 diffractometers, and 25 ellipsometers were developed at the ISP SB RAS.

The Katun' MBE system developed at the Institute and the 32P MBE system produced by the Riber Corporation were used to grow semiconducting III–V, IV–IV, and II–VI heterostructures to produce Gunn-effect diodes operating in the millimeter wavelength range (at a frequency of 28 GHz) [3], monolithic integrated circuits [4], GaAs–AlGaAs quantum-well matrix IR photodetectors [5], GaAs–InGaAs–GaAs high-power SHF transistors (2–18 GHz) [6], lasers with vertical resonators [7], silicon field-effect transisors with Ge dots in the channel [8], and HgCdTe [9, 10] and GeSi/Si photodetectors [11, 12] operating in the medium IR range (3–5 μm).

Schottky-barrier field-effect SHF transistors

Semiconducting layers studied in the present paper and AlGaAs/InGaAs/GaAs pseudomorphous heterostructures of SHF transistors were grown in the Riber 32P MBE system on GaAs semiinsulating plates with the (001) orientation. The field-effect transisors (FET) had the gate length $L_g = 0.5$ μm and the gate widths $W_{tr} = 180$ and 300 μm. Ohmic contacts, gate, and grooves of the trancated channel were patterned by electron-beam lithography using a ZBA-20 system. Au/Ge/Au ohmic contacts were patterned by pulsed annealing. Ti/Au was used for gate metallization. Bumps of the source electrodes 6–7 μm high, gate, and drain were grown in contact windows by galvanization. This enabled back bonding of integrated FET chips. The low-temperature SiO_2 ($T = 250$°C) was used as an interlayer dielectric. The mesa was insulated by implantation of B^+ ions. The groove of channel truncation simultaneously forming the gate was produced by wet chemical etching in an $H_2O_2 : H_3PO_4 : H_2O$ solution; the gate was formed by explosive technique.

Fig. 1 shows dynamic characteristics of FET manufactured on these plates. Both transistor types have wide dynamic ranges at positive gate biases up to +(1.5–2.0) V, when the peak drain current exceeds almost twice the saturation drain current at $U_g = 0$. The gate-drain breakdown characteristic of the pseudomorphous FET has a steep (avalanche) character, which confirms the low impurity content in the gate pseudo-dielectric.

Gunn diodes with the two-barrier injector of hot electrons and integrated circuits based on GaAs epitaxial films

The efficiency of application of $Ga_{1-x}Al_xAs$–GaAs heteroepitaxial injecting cathode junction in Gunn-effect diodes (GED) operating in the millimeter wavelength range (MWR) was demonstrated in many studies. The GED active element with the two-barrier $Al_{0.3}Ga_{0.7}As$–GaAs–$Al_{0.3}Ga_{0.7}As$ heteroepitaxial structure being an injector of hot electrons was developed at the ISP SB RAS in collaboration with the Federal State Unitary Enterprise Scientific-Research Institute of Semiconducting Materials (FSUE SRISM, Tomsk) [3] based on the achievements of molecular-beam epitaxy in the production of two-barrier (TB) AlAs–GaAs–AlAs heterostructures with high current density in the mode of resonant tunneling and thermal field emission to improve the dynamic and noise characteristics of the element in the region of negative differential resistance compared to the conventional GED and resonance-tunnel diodes in which the TB

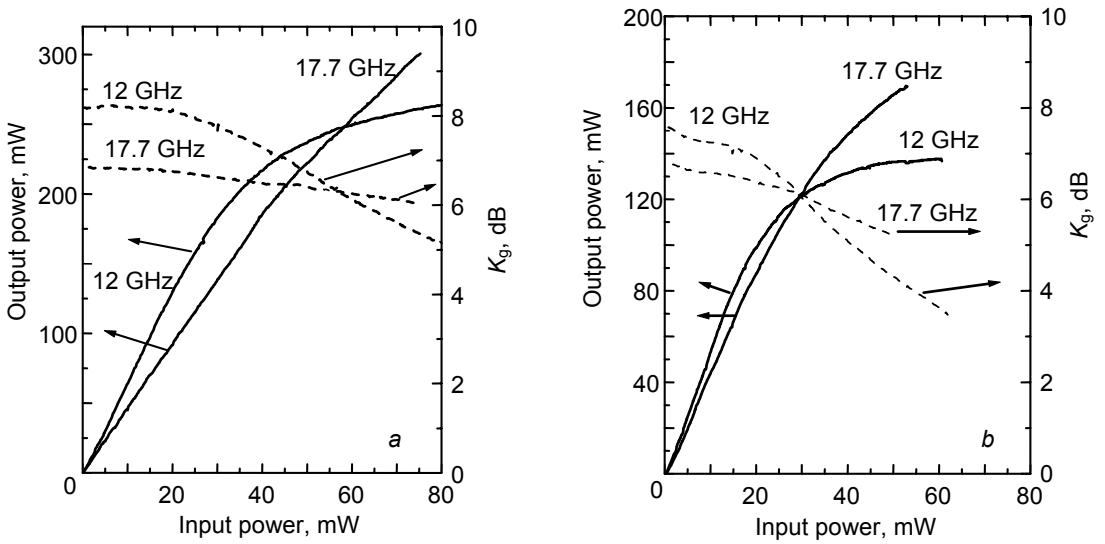

Fig. 1. Dependence of the output power and gain K on the input power at frequencies of 12.0 and 17.7 GHz for transistors based on structures with the gate dielectric layer of the thickness W_{tr} = 300 μm (*a*) and on pseudomorphous heterostructures with the thickness W_{tr} = 180 μm (*b*).

heteroepitaxial structure is surrounded by contact n^+-regions. This TB heteroepitaxial structure plays the role of fast-response ($\tau = h/\Delta E$) quantum-mechanical energy filter of injected hot electrons. Here h is Planck's constant and ΔE is the energy range for which the transmission coefficient of the TB heterostructure is halved compared to its maximum value in the resonance.

Conventional active GED elements were produced using the standard technology. Then the contact n^+-layer was stripped, and the two-barrier cathode $Al_{0.3}Ga_{0.7}As$–GaAs–$Al_{0.3}Ga_{0.7}As$ heterostructure and GaAs layers were formed in place of this contact layer. Epitaxy was conducted in a re-equipped chamber of the MBE system in a closed volume completely shielded by walls that were cooled with liquid nitrogen. The atomic purity of the active surface region $na(x)$ was first ensured. Then undoped *i*-GaAs (50 Å), $Al_{0.3}Ga_{0.7}As$ (25 Å), *i*-GaAs (50 Å), and $Al_{0.3}Ga_{0.7}As$ (25 Å) layers were grown successively at a temperature of 600°C followed by the GaAs contact region with a smooth transition from the low ($5\cdot10^{16}$ cm^{-3}) to high electron concentration ($2\cdot10^{18}$ cm^{-3}) grown at a temperature of 500°C. Undoped GaAs was grown with charge-carrier density of $(2–5)\cdot10^{14}$ cm^{-3} and mobility up to 8000 cm^2/(V·s). The LF and SHF characteristics of Gunn-effect diodes with active elements in the form of the two-barrier $Ga_{0.7}Al_{0.3}As$–GaAs–$Ga_{0.7}Al_{0.3}As$ heterostructure grown by molecular beam epitaxy in place of the stripped contact n^+-layer were compared for the long-wavelength portion of MWR at 300 and 77 K. For diodes with the injecting cathode contact, we observed the displacement of working frequencies corresponding to the maximum SHF power (more than 150 mW) toward lower frequencies, a noticeable increase in the efficiency (up to 6.4%), and stable operation at a temperature of 77 K compared to conventional GED [3].

Based on GaAs epitaxial structures, operating digital and analogue integrated circuits were manufactured. They are characterized by lower energy consumption, lower working voltages, and faster response compared to analogous structures based on ion-doped materials. The new technique of growing GaAs epitaxial films with the formation of a cold buffer layer has been developed to produce integrated circuits [4].

Vertical-resonator lasers

Over the past few years, progress in the development of semiconducting lasers has been largely determined by the design and creation of vertical-resonator lasers (VRL). Record parameters of the threshold current, current modulation

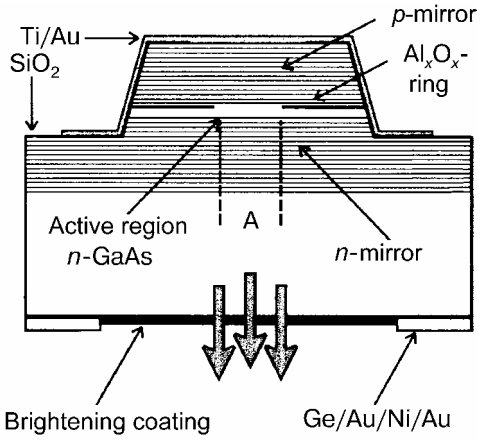

Fig. 2

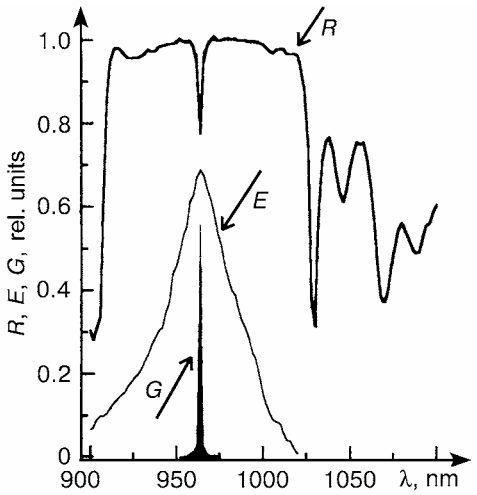

Fig. 3

Fig. 2. Scheme of the vertical-resonator laser.

Fig. 3. Reflection, electroluminescence, and generation spectra of the vertical-resonator laser.

frequency, and beam divergence obtained in VRL significantly extend the capabilities of semiconducting lasers and stimulate further research in this field.

This paper presents the results of investigations into lasing characteristics of optimized VRL with high external quantum efficiency and output power.

Initial laser structures were grown by molecular-beam epitaxy on the (001) GaAs n^+-substrates. The laser comprised undoped active regions of width λ, including three 8-nm $In_{0.2}Ga_{0.8}As$ quantum wells and *p*- and *n*-doped mirror regions forming the Fabry-Perot interferometer and consisting of multiply repeated λ/4 GaAs and $Al_{0.9}Ga_{0.1}As$ layers (20 and 22.5 periods for *p*- and *n*-mirrors, respectively). Charge carriers were injected into the active region through *p*- and *n*-mirrors. GaAs and $Al_{0.9}Ga_{0.1}As$ mirrors were doped to the concentration of $1 \cdot 10^{18}$ cm^{-3}. The top *p*-mirror was covered by a heavily doped GaAs<Be ~ $1 \cdot 10^{19}$ cm^{-3}> layer 47 nm thick functioning as a contact region and matching phases of optical beams reflected from the Ti (2 nm)/Au (120 nm) metal coating and semiconducting heterointerfaces. Figure 2 shows the VRL scheme. The VRL aperture (*A*) is determined by the inner diameter of the Al_xO_y ring produced by selective oxidation of AlAs layers. It was varied from 2 to 10^3 μm [7]. To do this, the 66-nm AlAs layer adjacent to the active region was used. VRL radiation was extracted through the GaAs substrate with a brightening coating.

Figure 3 shows the reflection spectrum *R* of the laser system together with electroluminescence (*E*) and VRL generation spectra (*G*). The experimental reflection spectrum agrees well with the calculated spectrum and contains the resonance of the Fabry-Perot interferometer around 965 nm, whose position coincides with the maximum of the electroluminescence spectrum. The VRL generation wavelength corresponds to the position of the interferometer resonance.

The high external differential quantum efficiency η_e of our VRL is ensured by the high inner quantum efficiency $h_i > 0.9$ and the optimal ratio of the mirror reflection coefficients: the top mirror has extremely high reflection coefficient R_t close to 1 (its calculated value is $R_t = 0.9992$), and the bottom (output) mirror has $R_b = 0.99$.

Output radiation of all VRL under study has the narrow directional pattern. For the VRL with the aperture $A = 3$ μm, the beam half-width at half-maximum was 4.7°, and for VRL with larger aperture, this parameter did not exceed 3°. It is remarkable that beams of high-power lasers with large working apertures also have narrow directional patterns.

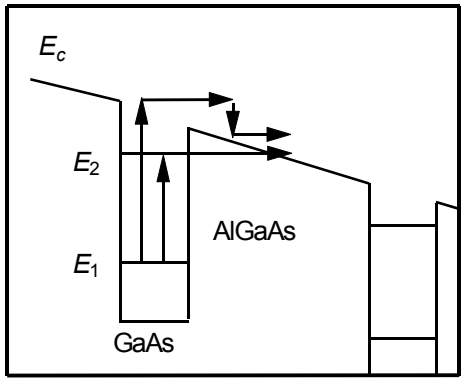

Fig. 4. Energy level diagram of the MSQW conduction band. Here E_1 and E_2 are quantizing levels for transverse electron motion and E_c is the edge of the conduction band of the bulk material. The arrows indicate possible electron transitions from the well after the photon absorption.

Photoelectric properties of structures with quantum wells

Due to highly homogeneous photosensitivity, multilayer GaAs/AlGaAs structures with quantum wells are the main type of photodetectors for wide-angle matrix thermal imaging systems operating in the wavelength range 8–12 μm. The quantum efficiency of photodetectors in this IR range is less important, since the accumulation time t_{acc} of thermal imaging systems with photodetectors having high quantum efficiency, as a rule, is much less than the framing time t_{fr} ($t_{acc} \sim 0.01\ t_{fr}$) because of limitations imposed by background illumination and the charge capacitance of input devices of silicon processors reading IR images. Therefore, photoelectric signal losses caused by the lower (by a factor of 5–10) quantum efficiency of photodetectors based on GaAs/AlGaAs structures with quantum wells compared to HgCdTe photodiodes can be completely compensated by increasing the accumulation time.

The 128 × 128 matrix photodetectors are a set of column photoresistors on a semi-insulating GaAs substrate with an n^+-GaAs common contact bottom layer 0.6 μm thick and an In bump on each resistive element to form the ohmic contact between the photodetector matrix and input cells of the silicon multiplexer to register photocurrent and to form a videosignal. A two-dimensional diffraction grating capped by the sealed ohmic GaAs contact is under the In bump in the n^+-GaAs contact layer 0.8 μm thick. The photodetector is illuminated from the substrate side.

Figure 4 shows the band diagram of the structure based on a multilayer system of GaAs quantum-dimensional wells (MSQW) and AlGaAs barriers (GaAs/AlGaAs MSQW). GaAs and AlGaAs layers have thicknesses of 4–5 and 40–50 nm, respectively. GaAs layers are doped with Si donor impurity to the concentration $N_{Si} \approx 3 \cdot 10^{17}$–$2 \cdot 10^{18}$ cm^{-3}. The photoconductivity of the system is determined by charge carriers excited directly from the bound ground energy level into states of the quasi-continuous spectrum above the barrier or by charge carriers excited into a bound energy level inside the well and subsequently tunneling to states of the quasi-continuous spectrum. Figure 4 shows the diagram of these transitions. The photodetector parameters (spectral behavior of the absorption coefficient, the detection threshold, and the dark current) depend on mutual positions of quantizing levels ε_n and the potential barrier (edge of the AlGaAs conduction band), the sweeping electric field, the working temperature, and the dimensions of the individual photodetector element. The $Al_xGa_{1-x}As$ composition is selected so that the level ε_2 is close to the edge of the barrier V_b and the condition $W(V) >> 1/t_{21}$ is satisfied. Here $W(V)$ is the tunneling probability, and $t_{21} \approx 10^{-13}$ s is the charge carrier lifetime on the excited level before emitting an optical photon.

Figure 5 shows a thermal image recorded with the MSQW GaAs/AlGaAs photodetector module having the maximum photosensitivity at a wavelength of 7.8 μm.

Fig. 5. Thermal image in the spectral range 5–8.5 μm.

CONCLUSIONS

Over the past few years, the ISP SB RAS in cooperation with the S. P. Korolev Energiya Rocket-Space Complex continues to improve the MBE technique. It has developed experimental systems and devices to implement MBE in the open space near the orbital station behind the molecular screen [13]. The E. O. Paton Institute of Electric Welding (Kiev) is now joining the Project aimed at removal of principal limitations of the MBE process to produce very high-quality structures using ground-based vacuum systems. Limiting factors here are the degree and purity of vacuum, throughput of the pumping system, and walls of the vacuum chamber accumulating and liberating molecular beam components and residual gas atmospheres. They can be removed by launching the technological system into a space orbit and subsequent operation behind the molecular screen [13–15]. According to the Program of Scientific-Applied Research of the Russian Segment of the International Space Station, the first experiments are planned for 2006. Now the ISP SB RAS is developing systems for space-born experiments and a stand imitating the outer space. It also studies the ground-based MBE processes and tests various parts of technological equipment.

REFERENCES

1. J. R. Arthur and J. J. LePore, J. Vac. Sci. Technol., **6**, 545 (1969); A. Y. Cho, J. Vac. Sci. Technol., **8**, 31 (1971).
2. A. Y. Cho, J. Cryst. Growth, **201/202**, 1 (1999).
3. A. I. Kurkan, T. A. Bannova, O. B. Koretskaya, *et al*., Elektronn. Promst, Nos. 1–2, 95 (1999).
4. V. V. Chaldyshev, M. A. Putyato, B. R. Semyagin, *et al*., *Ibid*., 154.
5. V. N. Ovsyuk, Yu. G. Sidorov, V. V. Vasilyev, and V. V. Shashkin, Appl. Phys., No. 5, 70 (2000).
6. K. S. Zhuravlev, A. I. Toropov, T. S. Shamirzaev, *et al*., Tech. Phys. Lett., **25**, No. 8, 595 (1999).
7. V. A. Gaisler, A. I. Toropov, A. K. Bakarov, *et al*., Tech. Phys. Lett., **25**, No. 10, 775 (1999).
8. A. I. Yakimov, C. J. Adkins, R. Boucher, *et al*., Phys. Rev., **B59**, No. 19, 12598 (1999).
9. Yu. G. Sidorov, S. A. Dvoretskii, V. S. Varavin, and N. N. Mikhailov, in: IR Matrix Photodetectors [in Russian], Nauka, Novosibirsk (2001), pp. 119–179.
10. V. V. Vasil'ev, Yu. G. Sidorov, S. A. Dvoretskii, *et al*., Avtometriya, No. 3, 4–8 (2001).
11. A. I. Yakimov, A. V. Dvurechenskii, and A. I. Nikiforov, Thin Solid Films, **380**, Nos. 1–2, 82 (2001).
12. A. V. Dvurechenskii, I. A. Ryazantsev, A. P. Kovchavtsev, *et al*., Prikl. Fiz., No. 2, 69 (2003).

13. O. P. Pchelyakov, A. I. Nikiforov, L. V. Sokolov, *et al*., in: Proc. 10th Symp. Physical Sciences in Microgravity, Vol. II, St. Petersburg (1997), p. 144.
14. A. Ignatiev, Earth Space Rev., **10**, 2 (1995).
15. V. I. Berzhatyi, L. L. Zvorykin, A. I. Ivanov, *et al*., Avtomat. Svarka, No. 10, 108 (1999).